Decomposition-Based Assembly Synthesis of Multiple Structures for Minimum Manufacturing Cost

Onur L. Cetin[1]
Graduate Student, Research Assistant

Kazuhiro Saitou[2]
Associate Professor
e-mail: kazu@umich.edu

Department of Mechanical Engineering,
University of Michigan, Ann Arbor, MI
48109-2125

An extension of decomposition-based assembly synthesis for structural modularity is presented where the early identification of shareable components within multiple structures is posed as an outcome of the minimization of estimated manufacturing costs. The manufacturing costs of components are estimated under given production volumes considering the economies of scale. Multiple structures are simultaneously decomposed, and the types of welded joints at component interfaces are selected from a given library, in order to minimize the overall manufacturing cost and the reduction of structural strength due to the introduction of joints. A multiobjective genetic algorithm is used to allow effective examination of trade-offs between manufacturing cost and structural strength. A new joint-oriented representation of structures combined with a "direct" crossover is introduced to enhance the efficiency of the search. A preliminary case study with two simplified aluminum space frame automotive bodies is presented to demonstrate that not all types of component sharing are economically justifiable under a certain production scenario. [DOI: 10.1115/1.1897409]

Keywords: Assembly Synthesis, Design for Modularity, Multiobjective Optimization

1 Introduction

Mechanical products are very rarely monolithic; one of the reasons is that the assembly of components allows simpler forms for the individual components, which are often more inexpensive to manufacture [1]. On the other hand, design for assembly (DFA) methodologies [2] often suggest the reduction of the number of components and joints to minimize the assembly cost. Furthermore, the structural products usually favor fewer joints, since very often joints are the weakest points: for instance, many fatigue failures are initiated from welded joints. The question is, therefore, "assuming a joint has to be made, what is the best method to do it?" [3]. Recognizing that the decisions on *where* and *how* the joints are to be made heavily impact the subsequent design processes of individual components, we have developed decomposition-based assembly synthesis [4,5], a method for the early identification of the joint locations and designs that minimally impact the overall structural strength.

Modular product design, which facilitates sharing components across multiple products, is viewed as a convenient way to offer high product variety with low manufacturing cost. The basic premise here is that the component sharing would result in less design effort and fewer production varieties with higher volumes, hence reducing overall manufacturing cost. As an extension of our previous work on decomposition-based assembly synthesis for structural modularity [6–8], this paper presents a preliminary attempt for the early identification of shareable components within multiple structures, posed as an *outcome* of the minimization of estimated manufacturing costs. The manufacturing costs of components are estimated under given production volumes considering the economies of scale. Multiple structures are simultaneously decomposed, and the types of welded joints at component interfaces are selected from a given library, in order to minimize the overall manufacturing cost and the reduction of structural strength due to the introduction of joints. A multiobjective genetic algorithm is used to allow effective examination of trade-offs between manufacturing cost and structural strength. A new joint-oriented representation of structures combined with a "direct" crossover is introduced to enhance the efficiency of the search. A preliminary case study with simplified aluminum space frame automotive bodies is presented to demonstrate that not all types of component sharing are economically justifiable under a certain production scenario.

2 Previous Work

2.1 Modular Design and Product Platform/Family. In the literature, a subsystem with common components and interfaces shared across product variants is often referred to as a product platform. As there are no fundamental conceptual and methodological differences between design for modularity and design of product platforms in the context of product family design, shared parts are consistently termed as modules instead of platforms in this paper, as in our previous work [6–8].

Similar to the classification in [9], we consider two different approaches for the solution of the design for modularity problem. In *two-stage approaches*, the first stage is devoted to optimally selecting modules, followed by the second stage of deriving each product variant for optimal performance utilizing the modules. Alternatively, *single-stage approaches* simultaneously determine the module and the resulting product variants for optimal performance of individual product variants as well as a product family. Despite the higher dimensionality, the single-stage approaches are the preferred method, since two-stage approaches require a priori selection of modules during the stage when the impact of the module selection on product performances is not explicitly known.

One of the earlier attempts of the single-stage design for modularity is by Fujita and Yoshida [10]. They first optimize the module selection and similarity among different products using a genetic algorithm, then optimize the directions of similarity on scale-based variety using branch-and-bound, and finally optimize the module attribute with sequential quadratic programing (SQP). Simpson and D'Souza [9] presented a mixed-integer programing

[1]Currently a post-doctoral research fellow, Engineering Design Centre, Cambridge University, UK.
[2]Corresponding author.
Contributed by the Design for Manufacturing Committee for publication in the JOURNAL OF MECHANICAL DESIGN. Manuscript received June 30, 2003; revised September 6, 2004. Associate Editor: D. Kazner.

formulation of the single-stage design for modularity problems where binary variables represent the selection of modules within a product family and continuous variables specify parameter values associated with each module. Fellini et al. [11] discussed a similar approach where the binary variables for module selection are relaxed to a continuously differentiable function that takes values in [0,1], to allow the use of gradient-based optimization algorithms. Extending the work of Simpson et al. [12], Messac et al. [13] introduced a product family penalty function to simultaneously maximize the performances of each design variant and minimize the variations in parameter values associated with chosen modules. These work, however, assume a predefined component topology in products under consideration. This often limits the applicability to structural products, since, because of their homogeneity, the determination of the component boundary (i.e., assembly synthesis) is inevitably an integral part of the identification of modular components.

Focusing on the application in structural design, we have developed a method for solving a single-stage approach for the design for modularity based on the decomposition-based assembly synthesis [6–8]. This method has been applied to two-dimensional (2D) continuum structures [8] and 2D [7] and three-dimensional (3D) beam structures [6], with special emphasis on the interface (joints) between modules and other components. The present work extends the method such that the optimal module design is achieved as an outcome of the simultaneous optimization of the performance of product variants and the manufacturing cost of a product family under particular production volumes.

2.2 Cost Estimation and Component Sharing. Since component sharing often results in a compromise in the performance of individual products, it is essential to quantify its effect on the overall manufacturing cost, in order to assess the trade-offs between cost savings and performance compromises.

Kim and Chhajed [14] developed an economic model that considers a market consisting of a high segment and a low segment. Greater commonality decreases manufacturing cost but makes the products more indistinguishable from one another, which makes the product more desirable for the low segment but less desirable for the high segment. Although the quality provided through the common design will yield the same utility, they report that there is a valuation change because of product similarity, which affects the perceived quality of products. On the supply side, cost savings will occur if a common modular design is used for the design of multiple products. This paper analyzes several sharing strategies using the cost model but does not suggest a rigorous solution for the optimization problem at hand.

Meyer et al. [15] proposed measurement methods of research and development (R&D) performance during platform design. One measure is called *platform effectiveness:* the degree to which the products based on a product platform produce revenue for the firm relative to the cost of developing those products. Mathematically, platform effectiveness considers R&D returns as accumulated profits divided by development costs, either at the individual product level or for groups of products within distinct platform versions. They presented a real-life application, but the method is used essentially for analysis of different sharing alternatives rather than as a tool during design.

Of special interest is the work by Fisher et al. [16] where they presented an analytic model of component sharing and show through empirical testing that this model explains much of the variation in sharing practice for automotive braking systems. The model takes as inputs a set of cars for which brakes must be designed and a set of possible design alternatives and determines which versions of each component should be built and which cars should use each component version to minimize cost. The cost functions model fixed and variable costs, and nonlinear production economies of scale. Similarly, Fujita and Yoshida [10] use a monotonic cost model for the assessment of benefits of commonality. The model consists of design and development cost (proportional to the weight of each module), facility cost (proportional to a representative attribute), and manufacturing cost (composed of material and processing costs). A learning effect is incorporated by reducing the manufacturing cost in accordance with an increasing number of production units due to commonality.

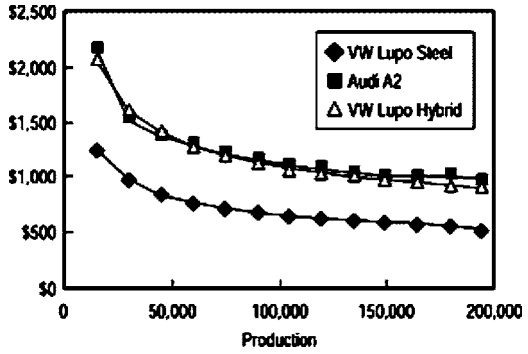

Fig. 1 Fabrication costs for several automobile body structures (from [18])

The specific cost-evaluation approach adopted in the case study of automotive aluminum space frames in Section 4 is based on the technical cost modeling method developed at the MIT Materials Systems Laboratory [17–19]. Kelkar et al. [17] report that the manufacture of the body-in-white is comprised of two costs: fabricating the parts and assembling the parts, with inputs of design specifications, material parameters, and production parameters. Inputs are transformed into estimates of fixed and variable costs for each manufacturing step. Variable costs include energy, materials, and direct labor; fixed costs cover capital equipment required for the manufacturing process, building expenses, maintenance, etc. They present the change of the average cost of each part with respect to production volume (such as the plot in Fig. 1), which indicates the main motivation for sharing modules in a family of products: it is possible to go down the curve by increasing the total production of the components and achieving considerable cost reduction.

3 Decomposition-Based Assembly Synthesis of Multiple Structures

3.1 Overview. The modular structural component design problem addressed in this paper is posed as an optimal selection of joint locations and joint types within n beam-based structures. Throughout the paper, *joint types* are referred to as the ways the beams are decomposed at a joint location, whereas *weld types* are the type of welding by which the decomposed beams are joined together, e.g., lap and butt welds. The approach can be summarized as follows:

- **Given:** n structures with loading conditions and their FEM results, possible joint locations, and production volumes
- **Find:** joint locations, joint types, and weld types in all structures
- **Minimizing:** reductions in structural strength because of joints and total manufacturing cost of all structures
- **Satisfying:** manufacturability of components

The n given structures are assumed to bear some similarity but are distinct in the geometry and/or loading conditions. Figure 2 shows a simple example of two such variant structures. Considering a mass-production environment, it is assumed that the reduction of manufacturing cost can be achieved by the improved component manufacturability as well as the increased production volume resulting from component sharing within variants.

For the given variant structures the designer defines the possible locations where a joint can be placed. Although the follow-

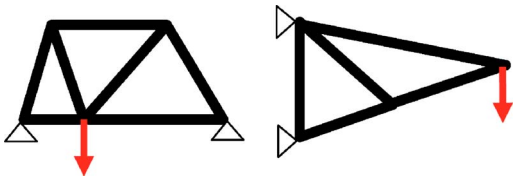

Fig. 2 Example of two beam-based product variants

ing examples simply assume joints can be placed at any intersections of beams in the structures, the designer may choose to allow joints to be placed only at some intersections or in the middle of some beams. For each possible joint location, the designer also must provide a *joint library*, feasible types of joints at the location, among which the optimal selection can be made. Figure 3 shows an example decomposition of the structures in Fig. 2, where the selected joint types are shown as numbers with the arrows indicating which beam is welded onto another. The two triangular components annotated with *s* are sharable components between the structures. Note that the sharable components identified automatically during the optimization, as a outcome of minimizing the overall manufacturing cost.

Although, overall, the steps of assembly synthesis described above is virtually identical to those found in [6–8], the distinct features of the present approach are (i) a new joint-oriented representation of structures, rather than topology graphs, which ensures the topological feasibility of decomposition without additional constraints, which, greatly simplifies the integration with a joint library; and (ii) the identification of sharable components as an *outcome* of minimizing the overall manufacturing cost, rather than simply maximizing the number of shared components. To quantify the cost reduction of component sharing (assumed to be primarily due to the economy of scale), production volumes of both variants are provided as an input to the cost estimation function; details are described in the following sections.

3.2 Definition of Design Variables. Let $L_k=\{1,2,\ldots,N_k\}$; $k=1,2,\ldots,n$ be the sets of possible joint locations in given structure k defined by the user. The design variables $\boldsymbol{x}_k$; $k=1,2,\ldots,n$ are the vectors of the *joint types* in structure i

$$\boldsymbol{x}_k=(x_{k1},x_{k2},\ldots,x_{kN_k}),\quad x_{ki}\in J_{ki},\quad i\in L_k,\quad k=1,2,\ldots,n \tag{1}$$

where J_{ki}; $k=1,2,\ldots,n$ are the sets of feasible joint types at location $i\in L_k$, of structure k, including a type specifying no joint. These sets are provided by the designer based on the material, manufacturing process and geometry of the structure. In the present study, joint types for all structures are defined as follows:

$$J_{ki}=\begin{cases}\{0,1,2\} & \text{if location } i \text{ is a two-beam intersection}\\ \{3,\ldots,14\} & \text{if location } i \text{ is at a three-beam intersection}\end{cases} \tag{2}$$

Joint types $0,\ldots,14$ are illustrated in Fig. 4, where joint type 0 corresponds to no joint and the arrows indicate which the beam is welded onto another. It is assumed a beam cannot be weld onto more than one beam. The beams from which the arrows are incident (the beams welding onto other beams) are referred to as the *welding beams*. Note that the three-beam intersection[3] must be always decomposed because branching beams cannot be manufactured with extrusion.

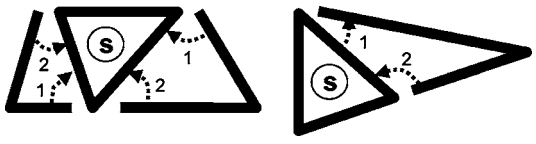

Fig. 3 Example of decomposition of the product variants in Fig. 2. The selected weld types are shown as numbers with the arrows indicating which beam is welded onto another. The identified sharable components are annotated with *s*.

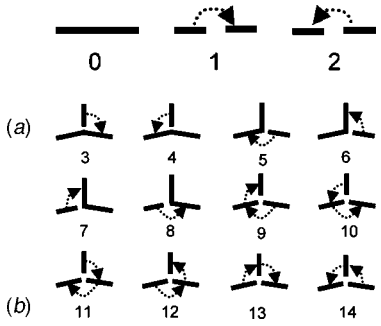

Fig. 4 Joint types of (*a*) two-beam intersection (types 0-2) and (*b*) three-beam intersection (types 3–14). The arrows indicate which beam is welded onto another. Note that three-beam intersection must be always decomposed since branching beams cannot be manufactured with extrusion.

Table 1 Weld types of extruded aluminum beams for space frame bodies [20]. Gray beams indicate the welding beams.

type	weld type	description	simplified representation
A	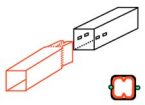	uniaxial	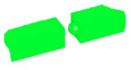
B	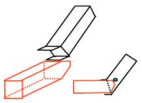	oblique	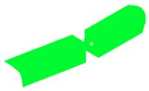
C	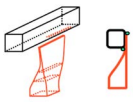	perpendicular lap	
D	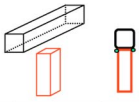	perpendicular butt	

Considering the application to automotive aluminum space frame (ASF) bodies, it is assumed that the structures are made of extruded aluminum beams joined via metal inert gas (MIG) or laser welding. As a preliminary attempt, each arrow in Fig. 4 indicates a weld of a type among the four weld types in Table 1 [20], where the gray (red in color) beam indicates the welding beam (the beam weld onto another beam). Note that only one weld type is possible if the joined beams are uniaxial (type A) and oblique (type B), whereas two weld types (types C and D) are possible between the beams perpendicular to each other.

In order to uniquely define the joint at a location, one must specify not only a joint type, but also a weld type. While design variables $\boldsymbol{x}_k$ specify a joint type at each possible joint location in structures k, a weld type is selected such that the weld will be subject to minimum force, as described in Section 3.3.

[3]No branch involving more than four beams are assumed in the structures.

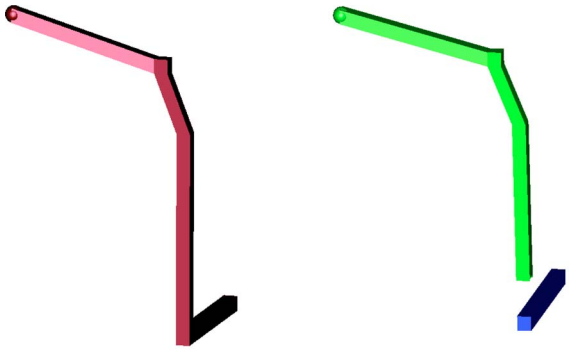

Fig. 5 (*a*) **infeasible component with an out-of-plane bend and** (*b*) **feasible components without out-of-plane bends**

3.3 Definition of Constraints. While joint types in Fig. 4 guarantee there will be no branching beams in a structure, it may still be possible for a component to have complex bends requiring sophisticated bending processes. Therefore, a manufacturability constraint is imposed to ensure that all components in a structure are "flat" without out-of-plane bends (to allow the use of simple bending dies), and the total angle of (in-plane) bends in every beam should not exceed 180 deg (to prevent potential obstructions during bending operation):

$$\text{FLAT}(\boldsymbol{x}_k) = \text{TRUE} \tag{3}$$

$$\text{OBSTRUCTIVE}(\boldsymbol{x}_k) = \text{FALSE} \tag{4}$$

where $k=1,2,\ldots,n$. Figure 5(*a*) shows an example of a component infeasible to the constraint (4), which can be made feasible, for example, by the introduction of an additional joint as shown in Fig. 5(*b*). Note this component is feasible to the constraint (4). The cost of in-plane bends in a structure is accounted for as a part of manufacturing cost, as discussed in Section 3.4.

3.4 Definition of Objective Functions.

3.4.1 Structural Strength. Since weld joints are the locations where fatigue failures are often initiated, their excessive use will reduce the overall structural strength. Dissimilar to spot welds that are much more susceptive to a tensile force than a shear force at the mating surfaces, the experimental results [21–27] suggest no such characteristics in MIG or laser welding. Assuming a similar weld length in each joint and forces on the mating surfaces (sleeves and flanges in Table 1) are carried by the beams themselves and not by the welds, the reduction of structural strength is estimated as the sum of the noncompressive forces at joints, as a first-order approximation suitable for conceptual design

$$f_S(\boldsymbol{x}_k) = \sum_{i \in L_k} F(x_{ki}) \tag{5}$$

where $k=1,2,\ldots,n$. $F(x_{ki})$ is the noncompressive force (with respect to the mating surfaces) at location i in structure k, which depends on the joint type x_{ki}. Obvisouly, $F(x_{ki})=0$ if $x_{ki}=0$ (no joint). Although sleeves and flanges in weld types A and B can significantly reduce the effect of moments at joints, it will not be the case for weld types C and D. Inclusion of the effect of moments in the estimation of structural strength reduction is left for the future work.

Noting that joint types 1–8 in Fig. 4 have only one weld whereas joint types 9–14 have two welds, $F(x_{ki})$ can be obtained by selecting the weld types in Table 1 that give the minimum force at the location

Table 2 Unit costs of bending and welding operation as a function of production volume [18,19].

q [10^4 units]	$c^w(q)$ [\$]	$c^b(q)$ [\$]
30	4.4	2.9
60	2.8	2.4
90	2.3	2.1
120	2.2	2.0
180	2.1	1.9

$$F(x_{ki}) = \begin{cases} \min\limits_{w \in W(x_{ki})} F_w & \text{if } x_{ki} \in \{1,\ldots,8\} \\ \min\limits_{(w,v) \in WV(x_{ki})} (F_w + F_v) & \text{if } x_{ki} \in \{9,\ldots,14\} \end{cases} \tag{6}$$

where $W(x_{ki}) \subseteq \{A,B,C,D\}$ is a set of feasible weld types of joint type $x_{ki} \in \{1,..,8\}$ at location i of structure k; $WV(x_{ki}) \subseteq \{A,B,C,D\}^2$ is a set of pairs of feasible weld types of joint type $x_{ki} \in \{9,..,14\}$ at location i of structure k; and F_w is the noncompressive force of weld type w in Table 1, given as

$$F_w = \begin{cases} |F^a| & \text{if } w \in \{A,B\} \\ \sqrt{\{\max(0,F^t)\}^2 + \{F^a\}^2} & \text{if } w = C \\ \sqrt{\{\max(0,F^a)\}^2 + \{F^t\}^2} & \text{if } w = D \end{cases} \tag{7}$$

where F^a and F^t are the axial and transversal forces on the welding beam. In Eq. (7), F^t for weld type C and F^a for weld type D are measured in the direction of the tension in the mating surface (i.e., compression is negative) in Table 1.

3.4.2 Manufacturing Cost. The cost of a structure consists of component cost and assembly cost. Since the introduction of joints does not change the total material used in a structure (the topology and dimensions of a structure are given) and extrusion is a low-cost process, it is assumed that component cost only depends on the cost of bending. Similarly, assembly cost is assumed to be only dependent on the cost of welding. Therefore, the total cost of producing one unit of each structures is given as

$$f_c(\boldsymbol{x}_1,\boldsymbol{x}_2,\ldots,\boldsymbol{x}_n) = f_c^w(\boldsymbol{x}_1,\boldsymbol{x}_2,\ldots,\boldsymbol{x}_n) + f_c^b(\boldsymbol{x}_1,\boldsymbol{x}_2,\ldots,\boldsymbol{x}_n) \tag{8}$$

where $f_c^w(\boldsymbol{x}_1,\boldsymbol{x}_2,\ldots,\boldsymbol{x}_n)$ and $f_c^b(\boldsymbol{x}_1,\boldsymbol{x}_2,\ldots,\boldsymbol{x}_n)$ are the total cost of welding and bending to produce one of each structure, respectively. The total welding cost is broken down into

$$f_c^w(\boldsymbol{x}_1,\boldsymbol{x}_2,\ldots,\boldsymbol{x}_n) = \sum_{k=1}^{n} c^w[(n_k^w - n_s^w)q_k](n_k^w - n_s^w) + c^w\left(n_s^w \sum_{k=1}^{n} q_k\right) nn_s^w \tag{9}$$

where $c^w(q)$ is the cost of a welding operation for production volume q; n_k^w, the number of welds in structure k (function of $\boldsymbol{x}_k$); n_s^w, the number of welds in the modules shared among structures $1,2,\ldots,n$ (function of $\boldsymbol{x}_1,\boldsymbol{x}_2,\ldots,\boldsymbol{x}_k$); and q_k, the production volume of structure k (user input).

The first term of Eq. (9) represents the sum of the costs of welds appearing only in structure k. The second term is the cost of welds in the modules shared in all structures. The breakdown of the total bending cost is given similarly (by replacing superscript w with b).

The unit cost of welding and bending operations $c^w(q)$ and $c^b(q)$, as a function of production volume q, are obtained by [18,19], respectively. Table 2 lists some of the actual values used in the calculation of Eq. (9), which exhibits a basic trend of economies of scale: exponential costs decrease similar to Fig. 1. Due to this trend, it is possible to reduce the cost of shared modules due to the increased production volume. Although the weld cost is higher than the bend cost at all production volumes, it

decreases more rapidly as the production volume increases, reaching to nearly the same amount as the bend cost at higher production volumes. The values (and the interpolations of them) in Table 2 are used for all weld types in Table 1, since the cost data in [18,19] are the average over typical weld operations.

To obtain the numbers of shared welds and bends, n_s^w and n_s^b, the components shared in all structures need to be identified first. This is done by checking the similarity of n components $\{c_1, c_2, \ldots, c_n\}$, each selected from n structures, and by repeating this check for all possible selections of components as specified by $\boldsymbol{x}_1, \boldsymbol{x}_2, \ldots, \boldsymbol{x}_n$. For each selection of n components, the similarity is checked by progressively applying the following criteria in the sequence:

1. Area of the bounding box (close within a given tolerance; 80% in the following case study)
2. Total bend angle (close within a given tolerance; 80% in the following case study)
3. Number of welds (identical)
4. Topology (identical)

The components $\{c_1, c_2, \ldots, c_n\}$ that passed all four criteria are considered as sharable in n structures and included in the calculation of n_s^w and n_s^b. The tolerances in criteria 1 and 2 control the degree to which n components are considered to be similar and hence sharable. These tolerances are adjusted to appropriate values in order to allow effective exploration of potential sharing options during the early design stages.

3.5 Formulation of Optimization Problem. The design variables, the constraints, and the objective functions defined in the previous sections provide the following biobjective optimization problem:

$$\text{minimize:} \quad \left\{ \sum_{k=1}^{n} f_s(\boldsymbol{x}_k), f_c(\boldsymbol{x}_1, \boldsymbol{x}_2, \ldots, \boldsymbol{x}_n) \right\}$$

subject to:

$$\text{FLAT}(\boldsymbol{x}_k) = \text{TRUE}; \; k = 1,2, \ldots, n$$

$$\text{OBSTRUCTIVE}(\boldsymbol{x}_k) = \text{FALSE}; \; k = 1,2, \ldots, n$$

$$\boldsymbol{x}_k \in J_{k1} \times J_{k2} \times \ldots \times J_{kN_k}; \; k = 1,2 \ldots, n \qquad (10)$$

Although weight can be assigned for each term $f_s(\boldsymbol{x}_k)$ in the first objective function, it is omitted in Eq. (10) for notational simplicity. For given production volumes of structures $1, \ldots, n$, this problem is solved using a multiobjective genetic algorithm (GA) as described in Section 3.6.

3.6 Optimization Algorithm. Due to its combinatorial nature, solving the above problem requires a discrete optimization algorithm. As such, a multiobjective genetic algorithm was chosen because of the robustness to discrete problems and efficiency in handling multiobjective problems without predefined weights or bounds on objective functions. The implementation used in the following case study is based on a nondominated sorting genetic algorithm (NSGA-II) [28,29], which dynamically determines an aggregate of multiple objective values of a solution based on its relative quality in the current population, as the number of other solutions dominating it in the current population. Readers should refer to [28,29] for details of the algorithm.

A new joint-oriented representation of structures described in Section 3.2 allows a chromosome (an internal representation of design variables in GA) to be simply a linear concatenation of $\boldsymbol{x}_1, \boldsymbol{x}_2, \ldots, \boldsymbol{x}_n$

$$\boldsymbol{c} = (\boldsymbol{x}_1, \boldsymbol{x}_2, \ldots, \boldsymbol{x}_n) \qquad (11)$$

In previous work [6–8], a design variable is assigned to an edge of the dual of topology graph of the structure, which causes a undesired many-to-one mapping between variables and decompositions. In the joint-oriented representation, on the other hand, there is a one-to-one mapping between the values of $\boldsymbol{x}_1, \boldsymbol{x}_2, \ldots, \boldsymbol{x}_n$ and resulting decompositions, facilitating a far more efficient search. The price is the added need of the complete enumeration of joint topology (as in Fig. 4), which depends on the topology of given structures. To further enhance the search efficiency of GA, a "direct" crossover scheme is adopted, which directly acts on phenotype (structures in 3D space in our case) rather than on genotype (a linear list of numbers in Eq. (11) in our case) as the conventional crossovers. As in [6], for each structure k this is achieved by

1. Select a random point within the bounding box of a parent structure and a random orientation.
2. Construct the plane that passes the point with the orientation.
3. Slice two parent structures with the plane and then swaping the resulting substructures to produce two offspring structures.

The crossover that directly operates on structures has an apparent advantage of preserving the local building blocks in the structures, which seems to significantly contribute to the improved search efficiency. Although some bias could be introduced in selecting a point and an orientation, uniform probabilities are used in the following case study. To further improve the search efficiency, a repair operator is applied to the offspring structures if they become infeasible to the manufacturability constraint in Eqs. (3) and (4). This is done, whenever possible, by enforcing the decomposition of an infeasible component into feasible ones. For example, an infeasible component in Fig. 5(*a*) can be decomposed to two feasible components in Fig. 5(*b*).

A software implementation of the optimization problem is done using the C++ programing language using the LEDA library from the Max-Planck Institute of Computer Science. ABAQUS software from the Hibbit, Karlson, and Savensen, Inc. is used for the finite element analyses. Multiobjective genetic algorithm code and visualization software for space frame structures are written by Karim Hamza and Byungwoo Lee respectively, at the Discrete Design Optimization Laboratory at the University of Michigan.

4 Case Study

4.1 Structural Models. This section describes a preliminary case study on two ($n=2$) simplified 3D aluminum space frame models under global-bending loading condition, as shown in Fig. 6. It is assumed that these frame designs are still preliminary with no consideration of component sharing (hence fairly different in geometry). The aim is to identify the options for potential component sharing that would results in the reduction of overall manufacturing cost, prior to the detailed design of each frame. Structure 1 (compact vehicle in Fig. 6(*a*)) is ~3.80 m in length (x direction), 1.70 m in width (y direction), and 1.55 m in height (z direction). Structure 2 (midsize vehicle in Fig. 6(*b*)) is approximately 5.00 m in length, 1.90 m in width, and 1.45 m in height. The geometries of these structures are modeled after the existing commercial vehicles, and are quite different each other. The tolerances for two components considered as similar are set to 80%, which is approximately an average difference of corresponding beams in both structures. Beams are modeled as hollow tubes with rectangular cross sections of 50×50 mm or 75×75 mm, with the wall thickness of 2 mm. The material is taken as a typical aluminum alloy with the modulus of elasticity of 74 GPa. Assuming left-right symmetry of component geometries, only a half body is modeled as shown in Fig. 6.

4.2 Production Volumes. To examine the impact of produc-

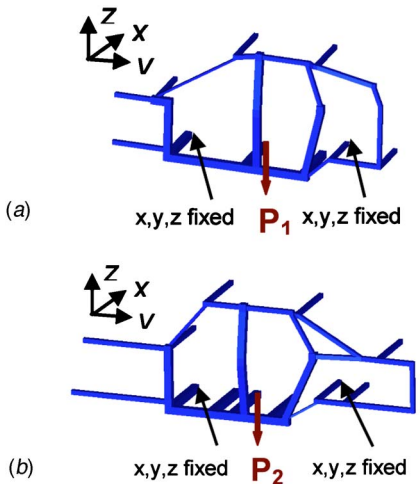

Fig. 6 Example aluminum space frame structures under global bending condition. (*a*) structure 1: compact vehicle subject to downward force P_1=895 kg and (*b*) structure 2: midsize vehicle with P_2=1770 kg.

tion volumes on the optimal decompositions, the following three scenarios of the production volumes are considered:

- **Scenario 1:** $(\nu_1, \nu_2)=(30{,}000, 30{,}000)$
- **Scenario 2:** $(\nu_1, \nu_2)=(90{,}000, 30{,}000)$.
- **Scenario 3:** $(\nu_1, \nu_2)=(90{,}000, 90{,}000)$

where ν_1 and ν_2 are the annual production volumes of structure 1 (compact vehicle) and structure 2 (midsize vehicle), respectively.

4.3 Optimization Results. Figure 7 shows the Pareto solutions of the three scenarios obtained by the multi-objective GA, where the horizontal and vertical axes are the sum of unit manufacturing costs of two structures $(f_c(\boldsymbol{x}_1, \boldsymbol{x}_2))$ and total forces on welds of two structures $(f_s(\boldsymbol{x}_1)+f_s(\boldsymbol{x}_2))$, respectively, as given in Eq. (10). Table 3 lists typical values of run-time parameters of GA used to obtain the result. The values are chosen to provide the results with good repeatability. Since functions $f_s(\boldsymbol{x}_1)$ and $f_s(\boldsymbol{x}_2)$ are evaluated by looking up the results of a single finite element analysis of each structure conducted prior to the optimization, the running time is approximately only 2 h with a 1.8 GHz PC.

The relative locations of the three Pareto solutions (elite populations at the 1000th generation) in Fig. 7 provide the following observations:

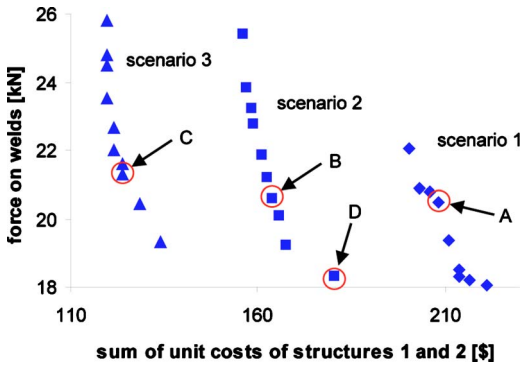

Fig. 7 Pareto optimal solutions for scenarios 1: (ν_1, ν_2) =(30,000,30,000), scenario 2: (ν_1, ν_2)=(90,000,30,000) and 3: (ν_1, ν_2)=(90,000,90,000)

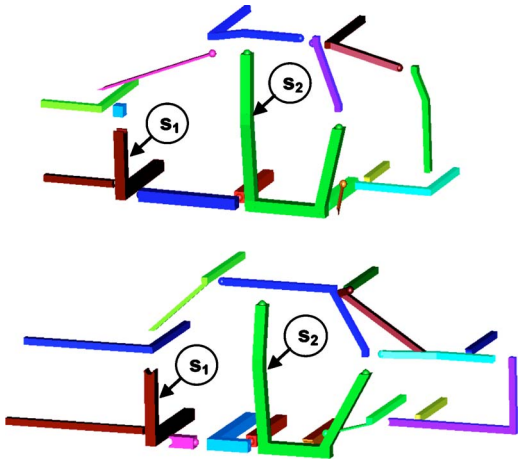

Fig. 8 Decomposed structures at point A in Fig. 7

- Manufacturing cost decreases (i.e., Pareto solutions shift to the left) as the production volume increases from Scenario 1 to Scenario 3. This is due to the reduction in costs of welding and bending at high production volumes.
- Force on welds increases (i.e., Pareto solutions shift up) as the production volume increases from Scenario 1 to Scenario 3. This is because of the increased preference of welds to bends for achieving low manufacturing cost at high production volumes.

In Scenario 1, welds are not desired at all as they are expensive and also increase the total force on welds, preferring complex components with multiple bends. This scenario also prefers modules since the effect of increased production volume on cost reduction is larger at smaller production volumes. In fact fewer modules are observed in Scenario 3 because of their minute effect on the cost reduction.

Figures 8–11 show the decomposed structures at points A, B, C, D in Figure 8, respectively, where weld types are represented graphically as shown in the third column of Table 1. Points A, B,

Table 3 Typical run-time GA parameters used in the case study

Population size	100
Number of generations	1000
Crossover probability	90%
Mutation probability	1%

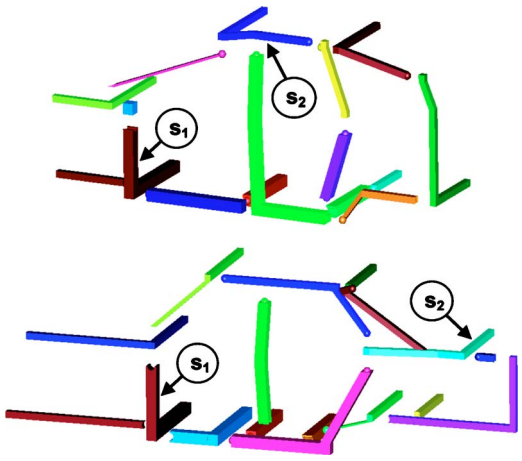

Fig. 9 Decomposed structures at point B in Fig. 7

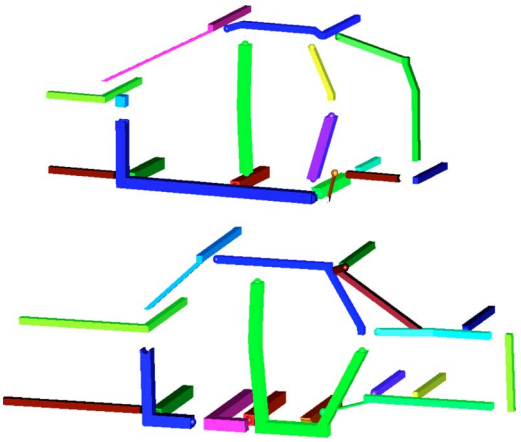

Fig. 10 Decomposed structures at point C in Fig. 7

and C are chosen from the "middle" of each Pareto curve to avoid the excessive bias to either one of the objective functions that tends to appear to the points near the ends of the curves. Point D is selected to isolate this bias for Scenario 2 and to be compared to Point B. Figure 8 shows the decomposed structures at point A (Scenario 1). The structures exhibit relatively small number of welds (i.e., complex components with multiple bends) and two shared modules, s_1 and s_2, both of which contribute to cost reduction under the production volumes of Scenario 1. Manual examinations of the decompositions corresponding to the other points in the Pareto set in Fig. 7 revealed that the same two modules appear at every point of the Pareto solutions, with the rest of the structures decomposed differently. It should be noted that some modules do not have exactly identical geometry. This is because two components are considered sharable if they are geometrically similar within predefined tolerances (80% in this case study) as stated in Section 3.4.2, to allow effective exploration of potential sharing options before the detailed design of each frame.

Figure 9 shows the results in point B (Scenario 2) that also contain two modules. Although module s_1 is identical to the one in Fig. 8, the large three-bend module in Fig. 8 is replaced by a small two-bend module (appearing in a rather creative fashion from the conventional body design viewpoint), due to the increased production volume of structure 1. Since there is very little cost reduction of having modules at high production volumes, no module appeared in the results of point C (Scenario 3) as seen in Fig. 10. This is also true for the other points for Scenario 3, except for the possibly random emergence of a few modules.

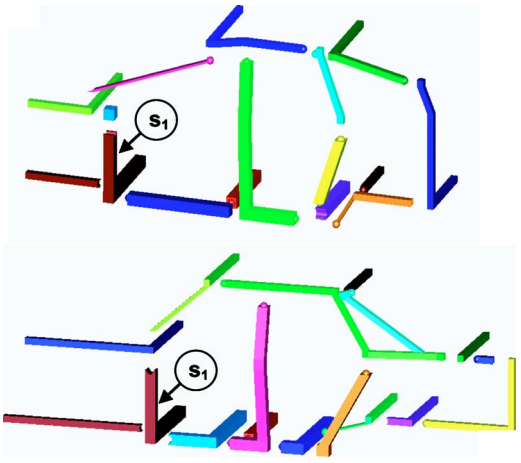

Fig. 11 Decomposed structures at point D in Fig. 7

Figure 11 shows the decomposed structure at point D (Scenario 2) with the minimum force on weld but maximum manufacturing cost. Since two structures are produced at different volumes in Scenario 2, there is a cost incentive to make a low-volume model (structure 2) similar to a high-volume model (structure 1). This can be observed by comparing the decompositions at point D (Fig. 11) and point B (Fig. 9). As the cost decreases from points B to D, the decomposition of structure 1 is kept constant, whereas the decomposition of structure 2 becomes more similar to structure 1 as indicated by the increased number of modules (from 1 to 2).

In all results, there is virtually no uniaxial joint since the decomposition of a straight member with no bends simply increases the force on the welds with no cost reduction. A relatively small number of identified modules is due to the tolerances (80%) in the similarity check described in Sec. 3.4.2, which might be tight for the two structures (modeled after existing vehicles) with not very similar dimensions.

5 Discussion and Future Work

This paper discussed an optimization-based method for simultaneous decomposition of multiple structures considering structural strength and manufacturing cost, where the identification of sharable modules is achieved as an outcome of minimizing manufacturing costs in a certain production scenario. A preliminary case study with two simplified automotive aluminum space frames demonstrated that the method can successfully quantify the effect of module sharing on structural strength and manufacturing cost by means of Pareto optimal solutions. Each Pareto optimal solution can be evaluated by a human decision maker before further design details are considered. Depending on the priorities with regard to strength and cost, solutions with balanced trade-offs (e.g., points A, B, C in Fig. 7) or extreme points (e.g., point D in Fig. 7) can be selected.

Not surprisingly, the effect of module sharing is negligible at larger production volumes (Scenario 3), as the economies of scale already provide a low cost for each component. On the other hand, modularity is an effective strategy at lower production volumes (Scenarios 1 and 2) for this specific application of space frame models. It should be noted, however, that the Pareto optimal solutions are quite sensitive to the unit cost of welds and bends and how they vary as a function of production quantity. Although this sensitivity is quite natural (as it is the cost that drives the decomposition), care should be taken on the accuracy of the cost model (refer to Table 2) to apply the present methods to products made with other manufacturing processes.

Although the results of the case study demonstrate the potential utility of the present approach, there are a number of refinements needed for it to be more practical. These include the refinement of structural strength evaluation, such as the inclusion of the moments on welds in Eq. (6); more strict similarity check, such as matching the force and moment at joints; and the identification of modules that are insensitive to the future changes in design details, such as dimensions. It is also of interest to incorporate a criterion on dimensional integrity, which is an important issue in welded beam assemblies. Although the method is fairly efficient (thanks to the simplified model of the structural strength that does not require repeated FEM runs during optimization), the scalability of the method in terms of the number of structures (i.e., for cases with $n>2$) and the complexity of each structure deserve further examination. In particular, difficulties are anticipated in the calculation of the component similarity because of the increased number of possible combinations of components. Therefore, a top-down hierarchical decomposition, from the entire structure down to substructures, can be a practical solution to manage the scalability issue. Furthermore, an explicit model of the gain of production flexibility and/or the changes in supply-side risk

should be added in order to better assess the benefit of using common components beyond a cost reduction. These extensions are to be reported at future opportunities.

Acknowledgments

O. L. Ceten has been partially supported by the National Science Foundation under CAREER Award (DMI-9984606), the Horace H. Rackham School of Graduate Studies at the University of Michigan, and General Motors Corporation through General Motors Collaborative Research Laboratory at the University of Michigan. These sources of support are gratefully acknowledged. The authors thank Dr. Donald Malen, for providing the joint library for aluminum space frames. Any opinions, findings, and conclusions or recommendations expressed in this material are those of the authors and do not necessarily reflect the views of the National Science Foundation.

References

[1] Gupta, S., Das, D., Regli, W. C., and Nau, D. S., 1997, "Automated Manufacturability: A Survey," Res. Eng. Des. **9**(3), pp. 168–190.

[2] Boothroyd, G., Dewhurst, P., and Knight, W., 1994, *Product Design for Manufacture and Assembly*, Marcel Dekker, New York.

[3] LeBacq, C., Brechet, Y., Shercliff, H. R., Jeggy, T., and Salvo, L., 2002, "Selection of Joining Methods in Mechanical Design," Mater. Des. **23**, pp. 405–416.

[4] Yetis, F. A., and Saitou, K., 2000, "Decomposition-Based Assembly Synthesis Based on Structural Considerations," *Proc. of 2000 ASME Design Engineering Technical Conferences*, Baltimore, Sept. 10–13, ASME, New York, ASME Paper No. DETC2000/DAC-1428.

[5] Yetis, F. A., and Saitou, K., 2002, "Decomposition-Based Assembly Synthesis Based on Structural Considerations," J. Mech. Des. **124**(4), pp. 593–601.

[6] Cetin, O. L., and Saitou, K., 2004, "Decomposition-Based Assembly Synthesis for Structural Modularity," J. Mech. Des. **126**(2), pp. 234–243.

[7] Cetin, O. L., Saitou, K., Nishigaki, H., Nishiwaki, S., Amago, T., and Kikuchi, N., 2001, "Modular Structural Component Design Using the First Order Analysis and Decomposition-Based Assembly Synthesis," *Proc. of 2001 ASME International Mechanical Engineering Congress and Exposition*, New York, Nov. 11–16, ASME, New York, ASME Paper No. IMECE2001/DE-23265.

[8] Cetin, O. L., and Saitou, K., 2004, "Decomposition-Based Assembly Synthesis for Maximum Structural Strength and Modularity," J. Mech. Des. **126**(2), pp. 244–253.

[9] Simpson, T. W., and D'Souza, B., 2002, "Assessing Variable Levels of Platform Commonality within a Product Family Using a Multiobjective Genetic Algorithm," *Proc. of 9th AIAA/ISSMO Symp. on Multidisciplinary Analysis and Optimization*, Atlanta, Sept. 4–6, AIAA, Washington, AIAA Paper No. AIAA2002-5427.

[10] Fujita, K., and Yoshida, H., 2001, "Product Variety Optimization: Simultaneous Optimization of Module Combination and Module Attributes," *Proc. of 2001 ASME Design Engineering Technical Conferences*, Pittsburgh, Sept. 9–12, ASME, New York, ASME Paper No. DETC2001/DAC-21058.

[11] Fellini, R., Kokkolaras, M., Perez-Duarte, A., and Papalambros, P. Y., 2002, "Platform Selection under Performance Loss Constraints in Optimal Design of Product Families," *Proc. of 2002 ASME Design Engineering Technical Conferences, Montreal*, Sept. 29–Oct. 2, ASME, New York, ASME Paper No. DETC2002/DAC-34099.

[12] Simpson, T. W., Maier, J. R. A., and Mistree, F., 2001, "Product Platform Design: Method and Application," Res. Eng. Des. **13**, pp. 2–22.

[13] Messac, A., Martinez, M. P., and Simpson, T. W., 2002, "Introduction of a Product Family Penalty Function Using Physical Programming," J. Mech. Des. **124**(2), pp. 164–172.

[14] Kim, K., and Chhajed, D., 2000, "Commonality in Product Design: Cost Saving, Valuation Change and Cannibalization," Eur. J. Oper. Res. **125**, pp. 602–621.

[15] Meyer, M. H., Tertzakian, P., and Utterback, J., 1997, "Metrics for Managing Product Development Within a Product Family Context," Manage. Sci. **43**(1), pp. 88–111.

[16] Fisher, M., Ramdas, K., and Ulrich, K., 1999, "Sharing in the Management of Product Variety: A Study of Automotive Braking Systems," Manage. Sci. **45**(3), pp. 297–315.

[17] Kelkar, A., Roth, R., and Clark, J., 2001, "Automobile Bodies: Can Aluminum Be an Economical Alternative to Steel?," J. Minerals Metals Mater. Soc. **53**(8), pp. 28–32.

[18] Constantine, B., 2001, "Economics of Tubular Hydroforming," Materials Systems Lab., Massachusetts Institute of Technology, Cambridge, MA, http://msl1.mit.edu/msl/meeting_04192001/prz_pdf/constantine.pdf

[19] Clark, J., 1998, "Future of Automotive Body Materials: Steel, Aluminum and Polymer Composites," Massachusetts Institute of Technology, Cambridge, MA, http://msl1.mit.edu/hoog. pdf

[20] Malen, D. E., 2002, *Course Notes from Fundamentals of Automotive Body Structures*, Dollar Bill Copying, Ann Arbor, MI.

[21] Cederqvist, L., and Reynolds, A. P., 2001, "Factors Affecting the Properties of Friction Stir Welded Aluminum Lap Joints," Welding J. Res. Suppl. **80**(12), pp. 281–287.

[22] Ye, N., and Moan, T., 2002, "Fatigue and Static Behavior of Aluminium Box-Stiffener Lap Joints," Int. J. Fatigue **24**, pp. 581–589.

[23] Matsumoto, T., and Izuchi, S., 1995, "Laser Welding of Aluminum Alloy Sheets," Kobe Steel Eng. Rep. **45**, pp. 72–74.

[24] Pinho da Cruz, J. A. M., Costa, J. D. M., Borrego, L. F. P., and Ferreira, J. A. M., 2000, "Fatigue Life Prediction in Almgsi1 Lap Joint Weldments," Int. J. Fatigue **22**, pp. 601–610.

[25] Behler, K., Berkmanns, J., Ehrhardt, A., and Frohn, W., 1997, "Laser Beam Welding of Low Weight Materials and Structures," Mater. Des. **18**(4–6), pp. 261–267.

[26] Matthes, K.-J., Lubeck, K.-H., and Lanzendorfer, G., 1998, "Influence of Irregularities at Butt-Welded Seams on the Behaviour of the Vibration-Fatigue Strength of Sheet-Aluminium Joints," Schweissen Schneiden **50**(3), pp. E57–E60.

[27] Ohta, A., and Mawari, T., 1990, "Fatigue Strength of Butt Welded Al-Mg Aluminium Alloy: Tests with Maximum Stress at Yield Strength," Fatigue Fract. Eng. Mater. Struct. **13**(2), pp. 53–58.

[28] Coello, C. A. C., van Veldhuizen, D. A., and Lamont, G. B., 2002, *Evolutionary Algorithms for Solving Multi-Objective Problems*, Kluwer Academic/Plenum Publishers, New York.

[29] Deb, K., Agrawal, S., Pratab, A., and Meyarivan, T., 2000, "A Fast Elitist Non-Dominated Sorting Genetic Algorithm for Multi-Objective Optimization: NSGA-II," *Parallel Problem Solving from Nature—PPSN VI*, M. Schoehaur, K. Deb, G. Rudolph, X. Yao, E. Lutton, J. J. Merelo, and H.-P. Schwefel, eds., Springer, New York, 1917, pp. 849–858.